Force Sensor Free Teleoperated Robotic Surgery

Interaction Force Estimation for Realistic
Force Feedback without Force Sensors

Edvard Nærum

Thesis submitted for the degree of philosophiae doctor

The Intervention Centre
Oslo University Hospital

Faculty of Medicine
University of Oslo

Series of dissertations submitted to the
Faculty of Medicine, University of Oslo
No. 1421

ISBN 978-82-8264-394-8

Cover: Inger Sandved Anfinsen.
Printed in Norway: AIT Oslo AS.

Produced in co-operation with Akademika publishing.
The thesis is produced by Unipub merely in connection with the
thesis defence. Kindly direct all inquiries regarding the thesis to the copyright
holder or the unit which grants the doctorate.

Acknowledgements

The research whose results are presented in this thesis was conducted between 2006 and 2011, at the Intervention Centre in Oslo, Norway. The Intervention Centre is a cross-disciplinary research department at the Oslo University Hospital, and it is a great environment for collaboration between medical personnel (doctors and nurses) and engineers in the search for new patient treatment methods within minimally invasive therapy. In 2008 I spent 11 months as a visiting researcher in the Biorobotics Lab at the University of Washington, in Seattle, USA. The Biorobotics Lab houses a group of highly talented students and faculty, dedicated to the development of new technologies for use in robotic surgery. My research has received funding from the Norwegian Research Council, and I want to thank them for giving me the opportunity to follow a great interest of mine; the application of technology within medicine in general, and the application of robotics within surgery in particular.

I would like to express my sincere gratitude to my supervisor, professor Ole Jakob Elle, with whom I have had countless conversations on topics such as robotics in medicine, challenges and potential solutions, research focus, article writing and many more. He has provided me with important technical and strategic advice and direction over the years we have spent together at the Intervention Centre. I would also like to thank my clinical supervisor, professor Erik Fosse. As an experienced surgeon and head of the Intervention Centre, he knows what it takes to succeed in a cross-disciplinary environment, and he has given me invaluable input and feedback on my research from a clinical viewpoint. Another colleague deserving of many thanks is Jordi Cornellà, who joined the Intervention Centre after finishing his doctoral degree in Barcelona. I have very much been enjoying working with Jordi, and his support and mathematical insight has helped me progress in my research efforts. Finally, I am grateful to have been given the chance to be a colleague of the people at the Intervention Centre. The mix of educational backgrounds is a source of many fulfilling discussions, and many of my colleagues have turned into personal friends. Also, thank you for willingly participating as test surgeons in my teleoperation palpation experiment. Friends and family outside the Intervention Centre also participated in the palpation experiment, and they deserve thanks as well!

Under the supervision of professor Blake Hannaford, the students in the Biorobotics Lab in Seattle show a great enthusiasm for their research, and the atmosphere is one of creativity and can-do attitude. I want to direct many thanks to professor Hannaford for his advice on robotics and teleoperation, without which many of my results would not have been possible. I want to thank Hawkeye King, for great times of collaboration in the lab, and perhaps even more for great friendship in general. I also want to thank Levi Miller for many a discussion on physics and maths, and equally for being a good friend. I miss the people of the Biorobotics Lab, and I very much appreciate having been given the opportunity to come and be part of their group.

By the start of 2010 I had collected all the data that were going to form the basis of my research, and I moved back home, into my dad's house, in order to put everything together. I am really grateful that I could come and stay with my dad and his wife, we had a good time together during the one year I was there. I was also able to finish the main body of my work in peaceful surroundings.

In January 2011 I started a new job. In February that same year I married my beautiful wife, Paola. During the first year of our marriage we have both been working full-time, and Paola has had to put up with a husband who many a day has also spent the entire evening working on his thesis. Paola, I cannot thank you enough for the patience you have had with me during the final stages of my PhD studies. You have supported me the whole time, and you have also helped me directly through your valuable feedback on my thesis and my papers. I love you Paola.

Edvard Nærum
Oslo, March 26, 2012

Contents

Chapter 1

Introduction

1.1 Teleoperated Robotic Surgery: Making Surgery Better

The beginnings of teleoperated robotic surgery date back only a little longer than a decade, to the end of the 1990's. Cardiac surgery was one of the main drivers behind the application of robotics to surgery. Miniaturized, dexterous instruments allowed surgeons to perform minimally invasive coronary artery bypass grafting and valve procedures [1]. The loss of dexterity was one of the most serious drawbacks of the keyhole surgery techniques that revolutionized surgical practice in the 1990's, and teleoperated robotic surgery was able to compensate for this loss. In keyhole surgery the surgeon operates through small incisions in the patient's skin, using purpose-built instruments. An endoscopic camera gives the surgeon eyes inside the patient. The instruments are shaped like a long, thin rod with a grasper, scalpel or similar at the tip. Operating endoscopic instruments is awkward and counter-intuitive, because of the pivot motion at the incision point and the inability to freely rotate the tip like a wrist. Suturing is an example of a task that is particularly difficult in keyhole surgery, as a result of the loss of dexterity. Consequently, the learning curve is steep for inexperienced surgeons. The articulated instruments of a surgical robot provides additional degrees of freedom in the shape of small wrists inside the patient, thereby largely restoring the dexterity of open surgery. Thus, the use of robots may lower the threshold for inexperienced surgeons to start performing keyhole surgery. Another important advantage of teleoperated robotic surgery is motion scaling. The scaling down of the surgeon's movements allows for surgical procedures to be carried out in cramped areas, where access with any type of manual surgery would be impossible, and with increased accuracy [2]. Furthermore, hand tremor may be filtered out in software, and the surgeon can sit in an ergonomically comfortable position while operating, instead of being stood by the operating table for several hours.

Up until today, only two systems for teleoperated robotic surgery have been commercially available. The *ZEUS*® system by Computer Motion (Goleta, CA, USA) and the *da Vinci*® system by Intuitive Surgical (Sunnyvale, CA, USA) were launched almost at the same time,

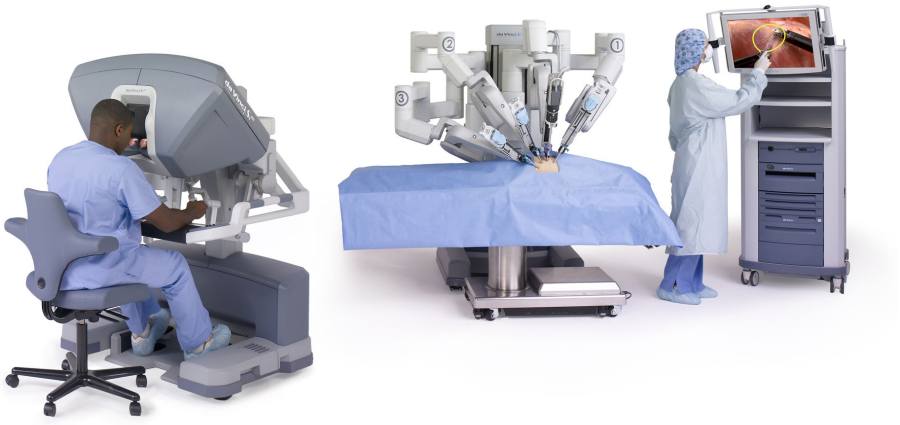

Figure 1.1: The components of the da Vinci system for teleoperated robotic surgery. The surgeon console (master robot) is on the left, while the patient-side (slave) robot is in the middle. © *2012 Intuitive Surgical, Inc.*

just before the turn of the millennium. Computer Motion was acquired by Intuitive Surgical in 2003, and the ZEUS system was discontinued shortly thereafter. Hence, the da Vinci system — shown in Figure 1.1 — remains the only system on the market. As of December 31st 2010, Intuitive Surgical had 1,752 of their da Vinci units installed in hospitals worldwide [3]. Although the surgeon console and the patient-side robot are physically separated, the *Food and Drug Administration* (FDA), which is responsible for the approval of new medical devices in the United States, requires that all procedures with the da Vinci system are performed with surgeon and patient located in the same room [1]. The most common use of the da Vinci system today can be found within the fields of gynecology and urology, with limited but increasing use in general surgery, otolaryngology, cardiac and thoracic surgery [4]. An example within urology is *radical prostatectomy* [5, 6]. In the United States 60-70% of the total number of radical prostatectomies are done robotically [7, 8]. Robot-assisted laparoscopic prostatectomy compares favorably with traditional open prostatectomy with respect to surgical margins, potency and continence [6], and with manual laparoscopic prostatectomy with respect to visualization, suturing and dissecting, and ergonomics [9].

For widespread adoption of teleoperated robotic surgery, simplicity and cost are important factors. In spite of Intuitive Surgical's growing base of da Vinci systems the use of teleoperated robots in surgery today is marginal. The technology is still in its infancy, and there are several limiting factors that impede its adoption. The acquisition of a system for teleoperated robotic surgery today is a considerable investment, and the large size of the robots makes them difficult to handle and increases setup time [1, 10, 11]. In addition, transmission delay for remote surgery [12] and the lack of haptic feedback [13] are limiting technological factors. These are discussed in more detail in Section 1.3. On the other hand, future technology will also unlock

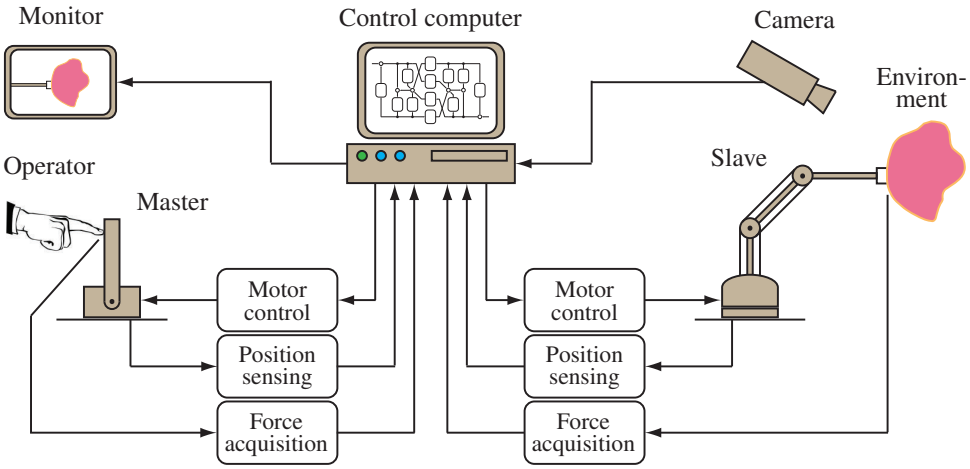

Figure 1.2: Overview of a bilateral teleoperation system. The vision subsystem (camera + monitor) is considered to be independent of the control software. Notice the symmetry of the signals communicated between master and slave manipulators.

new possibilities. Existing surgical procedures will be improved, and new procedures that are considered impossible today will become reality. Motion scaling will push frontiers and enable surgery in micro-scale and even nano-scale environments [14]. Automatic synchronization of the slave robot with moving organs such as the heart will make precision surgery like bypass grafting easier for the surgeon [15, 16]. Active shaping of human tissue characteristics and enhancement of perception with the help of intelligent teleoperation control software may equip the surgeon with super-human sensing capabilities [17, 18]. More stable, low-latency telecommunication lines will eventually allow the surgeon to be geographically separated from the patient.

1.2 Teleoperation at a Glance

The concept of *teleoperation* was invented in the late 1940's and was not at all related to surgery. Rather, the idea was conceived as a means of handling hazardous materials, such as nuclear waste [19]. The components of a teleoperation system is shown in Figure 1.2. A *human operator* manipulates the *master* robot, and the *slave* robot copies the motion at the remote site, possibly interacting with an *environment* or object of some sort. The master robot's position, and possibly the interaction force, is sensed, and a computer calculates the necessary motor control signals in order to make the slave copy the master motion. If the teleoperator is *bilateral*, then the same sense/control routine also takes place in the opposite direction. A bilateral teleoperator features haptic feedback, that is, the sense of touch and shape. If communication signals are only sent from master to slave, then the teleoperator lacks haptic feedback, and it is

said to be *unilateral*. A camera usually captures the action on the slave side, and the operator has visual contact via a monitor located on the master side. Strictly speaking, from a feedback control point of view the vision subsystem (camera + monitor) affects the behavioral characteristics of the overall teleoperation system, since the human operator's actions are based on the visual information on the monitor. Therefore, when the control software is designed, the whole system should be taken into consideration. However, vision is usually seen as an independent subsystem, and the control algorithms are designed assuming vision is not part of the feedback loop.

The original teleoperators were purely mechanical, but soon computers were employed to connect and control the master and slave robots electronically [20], like in Figure 1.2. Researchers have since spent decades in the quest to design computer programs that control the teleoperators in the best possible way. Traditionally two design keywords have been *stability* and *telepresence*. Stability is a fundamental requirement of any feedback control system, which a teleoperator ultimately is. Telepresence describes to what extent the operator feels present in the remote, but real, environment [21]. The word *transparency* is used to denote complete telepresence. A transparent teleoperator is 'invisible' to the operator, and manipulating the environment remotely is exactly identical to manipulating the environment directly. It is often pointed out that stability and telepresence are conflicting domains, and that teleoperation controller design is always a trade-off between the two [22, 23, 24]. The teleoperation literature may be classified according to that trade-off. On the one side can be found articles that focus on stability, using concepts such as robust control [25], passivity theory [26, 27], or absolute stability [28]. On the other side can be found articles that focus mainly on telepresence [29, 30, 31]. Teleoperated robotic surgery is subject to strict safety regulations. Thus, the stability requirement will have to be given special emphasis. Telepresence should be sought only while a generous stability margin can be preserved.

1.3 Clinical Challenges and Technical Bottlenecks

As mentioned in Section 1.1, there are multiple factors that impede widespread adoption of teleoperated robotic surgery. Among these are

- the cost of today's systems,
- the large size of the robots,
- transmission delay, and
- the lack of *haptic feedback* (sense of touch).

The bulkiness and large footprint of the da Vinci system results in the occupation of a lot of space next to the operating table. It also makes the system's mobility very poor. A lot of research is directed towards decreasing the size of the robots [32, 33, 34]. Transmission delay is

Figure 1.3: The EndoWrist instrument range used with the da Vinci system. © *2012 Intuitive Surgical, Inc.*

a problem that increases with the distance between surgeon console and patient-side robot, and it has been an active field of research for more than two decades [35, 36, 37]. In terms of feedback control, even small delays of a few milliseconds are a threat to the overall stability of the teleoperator. In addition, from a practical standpoint it is agreed that teleoperated surgery becomes infeasible for time delays larger than 200-300ms [38, 39], as the surgeon to an increasing extent has to actively consider the hand-eye coordination, adding another, tiring dimension to an already complex procedure. Even at the speed of light the round-trip delay between opposite ends of the earth is 130ms. Consequently, for the realization of remote surgery it is important to develop control algorithms that maintain stability of the teleoperator in the presence of delay, while at the same time achieve an acceptable level of usability for the surgeon.

Currently, teleoperated robotic surgery is performed unilaterally, that is, the surgeon receives no feedback from the operating site other than the visual information from the endoscopic camera. The lack of haptic feedback is largely due to the challenges associated with measuring the interaction forces between the surgical robot (slave) and the patient's tissue [40, 41]:

- Sensor size: The best interaction force measurements are obtained when the force sensor is mounted on the part of the instrument that is inside the patient's body, close to the tip. That imposes strict limitations on the size of the sensor. The diameter of the *EndoWrist*® instruments of the da Vinci system, shown in Figure 1.3, is 5mm or 8mm. Today there is no off-the-shelf force sensor of comparable size and with an adequate measurement range, although prototypes exist [42, 43, 44]. The size of the instruments in future teleoperated robotic surgery will also continue to decrease [45]. The force sensor may be placed on the instrument shaft outside the patient's body, where the size restrictions are acceptable, but friction forces at the instrument incision point and within the movable parts of the

instruments will severely distort measurements.

- Sensor cost: The measurement of forces also raises issues related to the cost of equipment, as integrated force sensors will make the surgical instruments more expensive. Alternatively, the sensors must be sterilizable for reuse, but that represents a design challenge that is hard to overcome.

As the implementation of haptic feedback is not a trivial task, numerous studies try to answer the question 'is haptic feedback really necessary in teleoperated robotic surgery?' A clear consensus is yet to be reached in the literature, although only rarely do studies conclude that the benefits of haptic feedback are negligible [46, 47]. Some argue that the visual clues provided by the excellent 3D vision of current robotic systems act as a substitute for haptic feedback [48, 49]. However, most of the work that directly compares surgical performance of teleoperated robots with and without haptic feedback concludes that it is helpful with respect to metrics like task completion time, peak force and the number of errors [50, 51, 52]. The benefits of haptic feedback are perhaps particularly evident for novice surgeons [53, 54].

With the presumption that the lack of haptic feedback does represent a real impediment for the widespread use of teleoperated robotic surgery, it is of great interest to find ways of restoring the sense of touch to the surgeon. The previously discussed problems of force measurement in robotic surgery encourage the search for alternate methods of implementing haptic feedback. One such method is *interaction force estimation*; the focus of this thesis.

1.4 Organization of the Thesis

Chapter 2 Presents the focus of the research and the research objectives pursued in the thesis.

Chapter 3 Describes the methods that are employed in order to respond to the research objectives.

Chapter 4 Summarizes the quantitative and qualitative results obtained from the experiments.

Chapter 5 Contains the general discussion of the contributions and results, with their advantages and limitations.

Chapter 6 Lists the main conclusions of the research.

Chapter 2

Focus of the Research

2.1 Force Feedback through Force Estimation

Haptic feedback can be divided into two categories, *force feedback* and *tactile feedback* [13]. Force feedback refers to the transmission of object shape or stiffness through the generation of motion or strain in the operator's muscles and joints. Tactile feedback refers to the transmission of touch and texture as felt by the human skin as a sensory organ. This thesis is concerned only with force feedback.

The control software of the first electronically controlled teleoperator generated force feedback based on the position error between the master and slave robots [19]. No force sensors are needed to implement that type of controller. However, the position-error-based controller performs poorly when aiming for a maximum degree of telepresence [55, 56]. Obtaining complete telepresence, or transparency, requires information about interaction forces in addition to the position of the robots [29]. It has also been shown that teleoperation controllers that are designed for maximum sensitivity rather than transparency benefit from the active use of interaction force information [57, 17]. That type of controller is particularly useful in robotic surgery, because it has the potential to improve the surgeon's perception threshold. In the absence of force sensors, interaction force information has to be obtained by *estimation*, utilizing other sources of available or measurable information. These sources typically include the position/velocity (also called *state*) of the robot, the torque applied by the robot's motors, and the robot's physical parameters. The focus of the research presented in this thesis is captured by the following phrase:

> *The estimation of interaction forces for the realization of force sensor free bilateral teleoperation with realistic or task-optimized force feedback for teleoperated robotic surgery.*

Interaction forces occur not only at the point of contact between the slave robot and the patient tissue, but also between the master robot and human operator. Although the slave force is most difficult to measure, we also pursue estimation of the master force. Task-optimized force

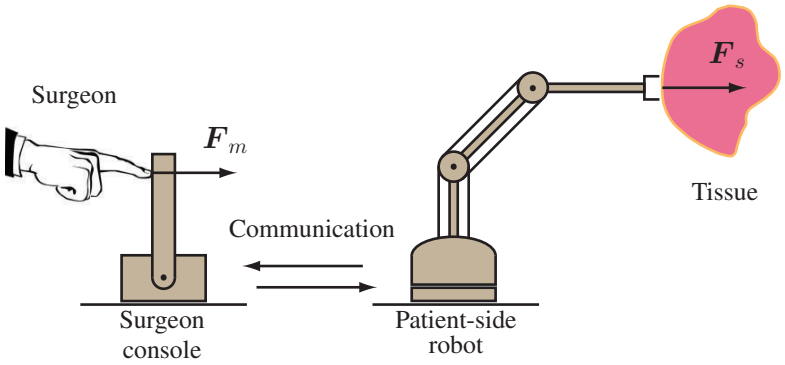

Figure 2.1: Bilateral teleoperation with interaction forces $\boldsymbol{F}_m$ and $\boldsymbol{F}_s$ and cable-driven slave.

feedback refers to the type of feedback that targets a specific surgical task. The manipulation of hard bone structures and the palpation of soft tissue are examples of tasks at opposite ends of the spectrum, and whose optimal type of feedback will differ.

2.2 Research Objectives

Figure 2.1 depicts a simplistic sketch of the principle of bilateral teleoperation, and it shows the points of contact where the interaction forces $\boldsymbol{F}_m$ and $\boldsymbol{F}_s$ occur. The sketch also shows a *cable-driven* slave robot. With reference to the sketch three major objectives are pursued:

1. Single point of contact: estimate $\boldsymbol{F}_s$. In teleoperated robotic surgery the slave robot is often cable-driven. That is also the case for the da Vinci robot. Due to the long and slender shape of the instruments used in keyhole surgery some or all of the motors have to be located away from the joint they actuate. Instead, motors and joints are connected by cables. Accurate interaction force estimation depends on the knowledge of the robot's physical parameters, but because of cable elasticity and complex cable friction, the parameters are hard to identify. Hence, the first research objective addresses the identification of the physical parameters of cable-driven robots, with emphasis on friction.

2. Dual point of contact: estimate $\boldsymbol{F}_m$ and $\boldsymbol{F}_s$. A bilateral teleoperator must be viewed as one system with two points of contact with its environment. At these points interaction forces occur simultaneously, and the forces are interdependent. When the operator applies a force $\boldsymbol{F}_m$ to the master manipulator, it directly affects $\boldsymbol{F}_s$, and vice versa. Consequently, the estimation of $\boldsymbol{F}_m$ and $\boldsymbol{F}_s$ cannot be done separately. The second research objective addresses the mechanisms of dual estimation in bilateral teleoperation.

3. Combine objectives 1 and 2 in the effort to accomplish the goal of force sensor free teleoperated robotic surgery with realistic or task-optimized force feedback.

Chapter 3

Methods

The sections of this chapter are divided corresponding to which of the three research objectives they respond to. Section 3.1 discusses interaction force estimation with a single robot, with emphasis on how to handle friction (objective 1). Section 3.2 discusses the mechanisms of dual interaction force estimation in bilateral teleoperation (objective 2). Section 3.3 combines the efforts of Sections 3.1 and 3.2 to form a task-optimized controller design method for teleoperated robotic surgery (objective 3).

3.1 Single Interaction Force Estimation

This section discusses the estimation of the forces that occur at the point of interaction between the end-effector of a cable-driven robot and its environment. The essence of the section is that *accurate interaction force estimation requires accurate parameter identification*. The identification of friction parameters is given special attention. Cable friction and cable elasticity are treated separately, and their combining is left as future work.

3.1.1 Basic Estimation Concept

A physical object obeys Newton's 2. law. The acceleration of the object times the mass of the object equals the sum of all forces applied to the object. That is formulated mathematically as

$$m\ddot{x} = \sum f \tag{3.1}$$

where m is the mass of the object, x is the position of the object and $\sum f$ is the sum of all forces applied to the object. Newton's 2. law also applies to more complex physical structures, like a serial-link robot with d joints or *Degrees of Freedom* (DoF). Figure 3.1 shows a robot with three DoFs. The variables q_1, q_2 and q_3 represent the joint angles of the robot, τ_{c1}, τ_{c2} and τ_{c3} are the torques applied to the joints by the motors, τ_{f1}, τ_{f2} and τ_{f3} are the friction torques that occur at each joint of the robot, and $\boldsymbol{F}_s$ is an externally applied force at the robot's end-effector. The

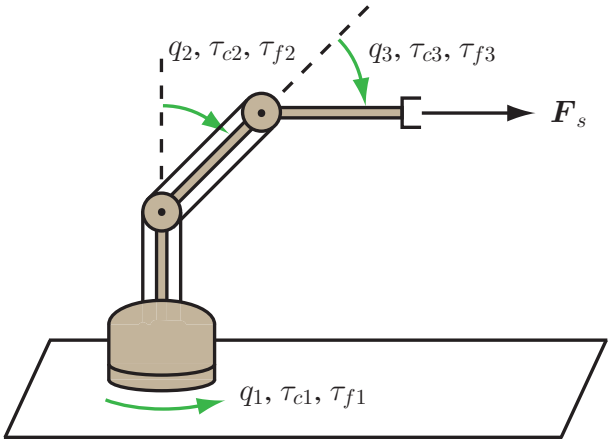

Figure 3.1: Serial-link robot with three Degrees of Freedom (DoF).

dynamic equation (Newton's 2. law) of the robot in Figure 3.1 is given by

$$\boldsymbol{M}(\boldsymbol{q})\ddot{\boldsymbol{q}} = \boldsymbol{\tau}_c - \boldsymbol{\tau}_f - \boldsymbol{C}(\boldsymbol{q}, \dot{\boldsymbol{q}})\dot{\boldsymbol{q}} - \boldsymbol{N}(\boldsymbol{q}) + \boldsymbol{\tau}_s \tag{3.2}$$

where $\boldsymbol{M}$ is the inertia (or mass) matrix, $\boldsymbol{q} = [q_1, q_2, q_3]^T$ is the joint angle vector, $\boldsymbol{\tau}_c = [\tau_{c1}, \tau_{c2}, \tau_{c3}]^T$ is the motor joint torque vector, $\boldsymbol{\tau}_f = [\tau_{f1}, \tau_{f2}, \tau_{f3}]^T$ is the joint friction vector, $\boldsymbol{C}$ is the Coriolis matrix, $\boldsymbol{N}$ is the gravity vector and $\boldsymbol{\tau}_s$ is the effective external joint torque vector, resulting from the application of $\boldsymbol{F}_s$. The two quantities are related through the manipulator Jacobian $\boldsymbol{J}(\boldsymbol{q})$ as $\boldsymbol{\tau}_s = \boldsymbol{J}^T(\boldsymbol{q})\boldsymbol{F}_s$. All the terms on the right-hand side of (3.2) together make up the sum of all forces applied to the robot.

The objective is to compute estimates of the externally applied force $\boldsymbol{F}_s$. Alternately, the corresponding torque $\boldsymbol{\tau}_s$ can be estimated, and $\boldsymbol{F}_s$ found via the manipulator Jacobian $\boldsymbol{J}$. The basis of force estimation throughout this thesis is the concept of *inverse dynamics* [58]. Roughly speaking, inverse dynamics means computing the forces applied to an object by measuring the motion of the object. In the case of the robot in Figure 3.1, it means that if the joint angle $\boldsymbol{q}$, the joint velocity $\dot{\boldsymbol{q}}$ and the joint acceleration $\ddot{\boldsymbol{q}}$ are known, then $\boldsymbol{\tau}_s$ can be computed as

$$\boldsymbol{\tau}_s = \boldsymbol{M}(\boldsymbol{q})\ddot{\boldsymbol{q}} + \boldsymbol{C}(\boldsymbol{q}, \dot{\boldsymbol{q}})\dot{\boldsymbol{q}} + \boldsymbol{N}(\boldsymbol{q}) + \boldsymbol{\tau}_f - \boldsymbol{\tau}_c. \tag{3.3}$$

That, however, also requires that $\boldsymbol{M}$, $\boldsymbol{C}$, $\boldsymbol{N}$ and $\boldsymbol{\tau}_f$ are known ($\boldsymbol{\tau}_c$ is the output of some control algorithm, and is therefore known). They must be found through *parameter identification*. The inertia matrix $\boldsymbol{M}$, the Coriolis matrix $\boldsymbol{C}$ and the gravity vector $\boldsymbol{N}$ may be found using for example a least-squares approach [59]. Here, focus is on the joint friction vector $\boldsymbol{\tau}_f$, whose estimation becomes more of a challenge in a cable-driven robot than in a regular robot. It is assumed during friction estimation that the cables are inelastic.

3.1.2 Estimation of Coupled Friction (Paper I)

Parameter identification refers to the process of finding the constant physical parameters that are contained in the dynamic equation of a system. Friction parameters are particularly difficult to identify, and most friction models are heuristic and do not accurately describe the underlying physical phenomena [60]. In a cable-driven robot, cables run from the base of the robot to the joint they actuate. If a cable actuates joint i, friction is created at joints $i-1$, $i-2$, ..., down to joint 1, due to the bending of the cable about the joint pulleys, imperfect pulley supports and misalignment between cable and pulley [61]. The total arrangement of cables thus creates a coupled friction picture. In teleoperated robotic surgery, the robots are usually operated at low velocities, where friction is predominant, complicating matters further. Friction forces may mask the delicate tissue interaction forces $\boldsymbol{F}_s$, thereby affecting the telepresence characteristics of the teleoperation system [62]. Hence, it is imperative to have an efficient friction model, with accurately identified parameters, so that friction can be compensated for.

The most common friction model used in engineering is the Coulomb+viscous model [59, 63]. However, numerous friction models have been developed in the attempt to capture complex friction phenomena, such as the Stribeck effect (increasing friction at low velocities), hysteresis, pre-sliding displacement and varying break-away force [64, 65, 66, 67]. The more advanced friction models are often dynamic, that is, the friction force is given as the output of a differential equation with one or more internal state variables. In contrast, static friction models (such as the Coulomb+viscous model) have no internal state variables. Instead, the output of the friction model is given as a function of velocity, and possibly other variables as well. A drawback of the Coulomb+viscous model, and all other friction models that are based on a predetermined structure, is that they cannot describe friction phenomena that are not captured by that specific structure. Examples of estimation techniques that *do not* make a priori assumptions about the structure of the friction model include neural networks [68, 69], fuzzy systems [70] or combinations thereof [71], and models that employ them are named *learning models*. The parameters of a neural friction model are identified through a training procedure where experimental data are used by the neural network to 'learn' how to reproduce the friction forces. A learning model also extends naturally to multiple dimensions, such that the friction model can have multiple inputs. That makes it suitable for use with a cable-driven robot, since the friction in one joint is a function of the motion of multiple joints along the robot's chain of links. In Paper I a *wavelet neural network* is proposed for the estimation of the coupled joint friction in a cable-driven robot. Like the Coulomb+viscous model, a wavelet network is *linear in the parameters*, which means that all the parameters of the model can be collected into one vector. Linearity in the parameters is favorable because it ensures ease of analysis and rapid parameter learning [72]. Unlike the Coulomb+viscous model, a wavelet network can approximate any static function (such as friction) to a desired accuracy [73]. Hence, a wavelet network model is a tool suitable for multi-dimensional friction estimation, it should outperform other static friction models

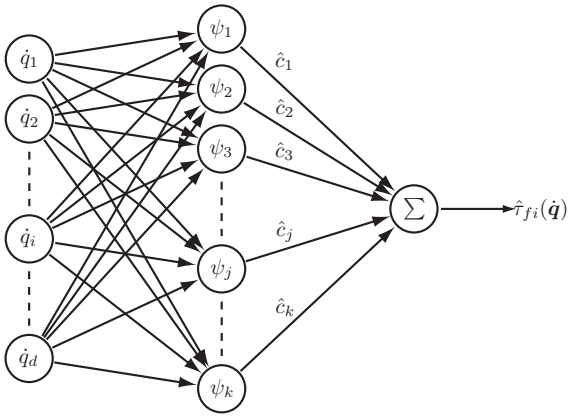

Figure 3.2: Graphical illustration of a wavelet neural network friction model.

in terms of estimation accuracy, and it is mathematically as simple as the Coulomb+viscous model.

The proposed wavelet network model computes the friction estimate $\hat{\tau}_{fi}$ of the ith joint of the robot as

$$\hat{\tau}_{fi}(\dot{\boldsymbol{q}}) = \sum_{j=1}^{k} \hat{c}_j \psi_j(\dot{\boldsymbol{q}}) \tag{3.4}$$

where the ψ_j are wavelets and the $\hat{c}_j$ are the model parameters. All the wavelets are offspring of one particular mother wavelet, and a special scheme is adopted from Sanner and Slotine [74] to dynamically pick the most suitable wavelets to be included in the network during learning. A Lyapunov-based approach is taken to develop an adaptation law that ensures proper identification of the $\hat{c}_j$ parameters [75]. Figure 3.2 shows how the wavelet friction model for each joint is a neural network comprising one hidden layer with k nodes and weights, d inputs and one output. The model of Figure 3.2 is implemented for every joint, and the overall joint friction estimate $\hat{\boldsymbol{\tau}}_f$ is constructed as $\hat{\boldsymbol{\tau}}_f(\dot{\boldsymbol{q}}) = [\hat{\tau}_{f1}(\dot{\boldsymbol{q}}), \hat{\tau}_{f2}(\dot{\boldsymbol{q}}), ..., \hat{\tau}_{fi}(\dot{\boldsymbol{q}}), ..., \hat{\tau}_{fd}(\dot{\boldsymbol{q}})]^T$.

The wavelet network friction model is tested using a 3-DoF PHANTOM Omni haptic device (Sensable Technologies, MA, USA). Ideally, the performance of the model should be evaluated by comparing measured friction to estimated friction. In general, friction as an isolated quantity cannot be measured. Hence, the performance of the wavelet network model is evaluated by computing the joint motor torque estimation error $\boldsymbol{e}_c := \boldsymbol{\tau}_c - \hat{\boldsymbol{\tau}}_c$ as an alternate performance metric. The estimated joint motor torque $\hat{\boldsymbol{\tau}}_c$ is computed by solving (3.2) with respect to $\boldsymbol{\tau}_c$, and its accuracy depends on the accuracy of $\hat{\boldsymbol{\tau}}_f$. The Omni is operated in free space during data collection, so $\boldsymbol{\tau}_s = \boldsymbol{0}$.

3.1.3 Parameter Identification by Manual Excitation (Paper II)

The field of robotic force control deals with the problem of maintaining a desired force in the interaction point between the robot's end-effector and its surroundings, and reliable interaction force information is essential. Typical applications include assembly, grinding and deburring [76]. Several approaches have been employed for the estimation of interaction forces in robotic force control, among them inverse dynamics [77, 78], disturbance observers [79], Kalman filter-like observers [80, 81] and vision-based observers [82]. At the moment it is not important what estimation approach is used, as all of the above approaches require parameter knowledge of some extent. Focus is therefore on accurately identifying the parameters contained in the robot's dynamic equation (3.2). That is often done by utilizing the joint motor torque estimation error $\boldsymbol{e}_c = \boldsymbol{\tau}_c - \hat{\boldsymbol{\tau}}_c$ in order to drive the parameters toward their correct values (as well as to evaluate performance, as in Paper I). In Paper II it is proposed to use the externally applied force $\boldsymbol{F}_s$ (or equivalently, $\boldsymbol{\tau}_s$)[1] during identification of $\boldsymbol{M}$, $\boldsymbol{C}$ and $\boldsymbol{N}$ instead of the motor torque $\boldsymbol{\tau}_c$. The friction torque $\boldsymbol{\tau}_f$ is estimated with the wavelet network model proposed in Paper I. The interaction torque estimation error $\boldsymbol{e}_s := \boldsymbol{\tau}_s - \hat{\boldsymbol{\tau}}_s$ is a *direct* measure of how well interaction forces can be estimated, whereas the motor torque estimation error $\boldsymbol{e}_c$ is only an indirect measure. With reference to Figure 3.1, external force data is collected by manually grasping the tip of the robot and moving it around in space, generating a series of $\boldsymbol{F}_s$ data. This technique for generating robot motion is named *manual excitation*. Manual excitation was also used by Smith et al. in [78]. However, they modeled the whole dynamic equation of the robot with a neural network, not just friction. It is our belief that learning models should be utilized only when physical modeling is infeasible.

Manual excitation has another two important advantages, in addition to the direct link between using $\boldsymbol{e}_s$ and interaction force estimation. The first advantage relates to the question of whether the motor torque vector $\boldsymbol{\tau}_c$ can be considered known, which is required when $\boldsymbol{e}_c = \boldsymbol{\tau}_c - \hat{\boldsymbol{\tau}}_c$ is used for parameter identification. Motor torque is a value set in the control software, and it is assumed that the actual torque applied at the joints will have the same value. In practice, this assumption hinges on a chain of conversion factors being correct, such as the motor's current-to-torque constant and the gear ratio. When manual excitation is used, the identification of this chain of conversion factors can be integrated into the overall parameter identification problem, and any incorrect conversion can be corrected. The second additional advantage of manual excitation relates to the training of the wavelet friction model (3.4). Learning models rely on having training data that appropriately reflect normal operating conditions. It means that the wavelet friction model (3.4) must be trained for all possible velocities $\dot{\boldsymbol{q}}$ that may occur during normal operation. In practice that cannot be achieved. However, since the motion of the human hand is naturally random, manual excitation will provide training data that are much richer than when motor torques make the robot follow a predetermined pattern.

[1] In Paper II the variable names $\boldsymbol{F}_e$ and $\boldsymbol{\tau}_e$ are used in place of $\boldsymbol{F}_s$ and $\boldsymbol{\tau}_s$, respectively.

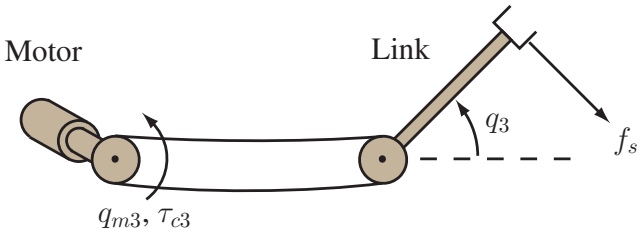

Figure 3.3: Single-DoF elastic transmission.

For the validation experiments the PHANTOM Omni is again used, only now fitted with an adapter that allows a force sensor to be attached at its tip for the recording of the force $\boldsymbol{F}_s$. Different from Paper I, the interaction torque estimation error $\boldsymbol{e}_s$ is used to evaluate the performance of the manual excitation algorithm in Paper II.

3.1.4 Estimation in Robots with Elastic Cables (Paper III)

Up until now it has been assumed that the cable transmission is inelastic. If the cables that run between motor and link are sufficiently short, that assumption may be justified. However, in a lot of cable-driven robots the cables are too long that their elasticity can be ignored. When the cables are elastic, the angle of the motor and the actuated link are slightly offset. Often only motor angle is measured. Consequently, the overall configuration of the robot cannot be computed, because the link angles are unknown. In turn, that means that it is not straightforward to apply inverse dynamics for interaction force estimation, since inverse dynamics rely on the complete motion (also called *state*) of the robot being known. Parameter identification and state estimation in robots with elastic transmissions have been extensively studied, using various methodologies to approach the problem [83, 84, 85, 86, 87]. In Paper III, simultaneous parameter identification and state estimation is undertaken for a 1-DoF elastic transmission, with only motor-side angle measurements available. That is a realistic situation in a lot of robots. Interaction force estimation is also studied in the same setting.

Figure 3.3 shows a stylized illustration of the third joint/link of the robot in Figure 3.1, where the link is actuated via an elastic transmission system. Due to the elasticity, separate variables are required to describe the motion on the motor and link side of the transmission; q_{m3} and $\dot{q}_{m3}$ for the motor-side state, and q_3 and $\dot{q}_3$ for the link-side state. Only q_{m3} is known, in addition to the motor torque τ_{c3}. Notice that f_s is used in place of $\boldsymbol{F}_s$ to indicate that the system in Figure 3.3 is 1-dimensional. An *Unscented Kalman Filter* (UKF) [88, 89] is employed to estimate the unknown state variables $\dot{q}_{m,3}$, q_3 and $\dot{q}_3$, and to identify the unknown physical parameters. The unknown parameters are the cable elasticity and the friction on both sides of the transmission. The only inputs to the UKF are the motor-side angle q_{m3} and the motor torque τ_{c3}. The simple Coulomb+viscous model is used in place of the wavelet friction model from Paper

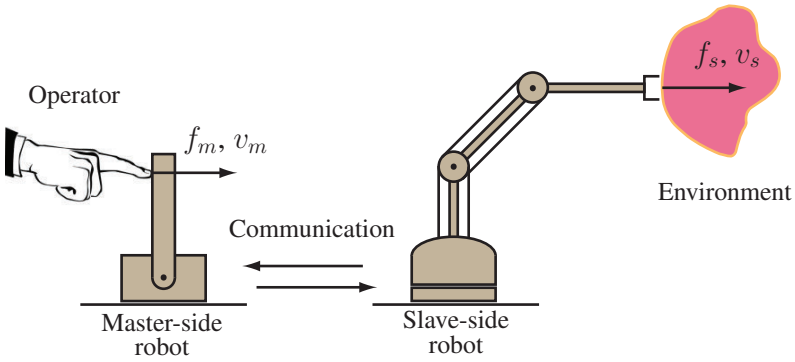

Figure 3.4: Bilateral teleoperation with interaction forces f_m and f_s, and velocities v_m and v_s.

I. The wavelet friction model is primarily developed for coupled friction phenomena, which is not an issue for the 1-DoF system in Figure 3.3. Wavelets still have the potential of outperforming the Coulomb+viscous model even for 1-DoF systems, and the training of wavelet networks inside a UKF algorithm is possible [90]. Yet, the inclusion of wavelet networks for friction estimation in elastic transmissions has been left for future studies. The UKF is chosen because simultaneous parameter identification and state estimation can be done through a straightforward implementation of the basic algorithm. Furthermore, the UKF is chosen over the *Extended Kalman Filter* (EKF) because it is capable of performing nonlinear estimation without linearization. The UKF has been used successfully in robotic applications [91] as well as non-robotic applications [92, 93].

Unlike Papers I and II, focus is here on state estimation and the elasticity of the cables, rather than interaction force estimation and the friction present in the system. In addition to testing the accuracy of the UKF's state and parameter estimates, Paper III studies the robustness of the UKF's state estimates when presented with variations in the transmission's inertia, cable tension and applied interaction forces during operation (when parameter identification has been switched off). Interaction force estimation with partial state knowledge is also studied within the same setting. The experiments are conducted using a 1-DoF cable transmission testbed.

3.2 Dual Interaction Force Estimation

In bilateral teleoperation there are two points of energy exchange; between the slave robot and its environment, and between the master robot and the operator. This section deals with the simultaneous estimation of the forces f_m and f_s that arise at these interaction points of a 1-DoF teleoperation system, shown as arrows in Figure 3.4. The figure is a copy of Figure 2.1, except that f_m and f_s are used in place of $\boldsymbol{F}_m$ and $\boldsymbol{F}_s$, since only 1-DoF systems are considered at the moment. The extension to multi-DoF systems is treated in Section 3.3. The essence of the section is that *the estimation of master and slave interaction forces in bilateral teleoperation*

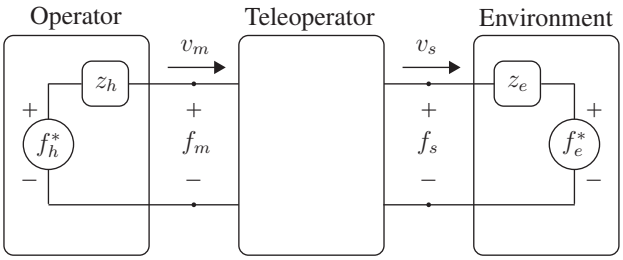

Figure 3.5: Two-port model of a bilateral teleoperator.

must be viewed as one problem.

3.2.1 The Modeling Basics of Bilateral Teleoperation

Since there two points (or ports) of energy exchange, a 1-DoF bilateral teleoperation system is often modeled as a *2-port network* [94]. Figure 3.5 shows the 2-port network that corresponds to Figure 3.4, where f_m and v_m are the force and velocity at the port connecting the master robot and the human operator, and f_s and v_s are the force and velocity at the port connecting the slave robot and the environment. The dynamics of the operator and environment are represented by the impedances z_h and z_e, respectively, and f_h^* and f_e^* are the intended forces. The 'Teleoperator' block contains the dynamics of the master and slave robots, plus all dynamics added as a result of implementing a particular teleoperation controller. In general the robot dynamics as well as the controller may contain both linear and nonlinear components. For the purpose of mathematical modeling some classification is convenient. We define two classes of teleoperators according to the degree of nonlinearity of its components:

Class I: The force and velocity variables all appear linearly in the dynamic equations, i.e., an overall linear teleoperator.

Class II: The force variables appear linearly in the dynamic equations, but the velocity variables may appear within nonlinear terms.

Notice that Class I is contained in Class II. Although classes may also be defined for even more general teleoperation systems, it is our claim that the large majority of teleoperators are covered by Class II.

The mathematical analysis of a Class I teleoperator is often done in the frequency domain. Because all signals appear linearly, a Class I teleoperator may be put on the form of the *Extended Lawrence Architecture* (ELA). The ELA is our name for the architecture originally devised by Lawrence [29], and later improved upon by Hashtrudi-Zaad and Salcudean [95]. The ELA is shown in Figure 3.6, and besides the operator and environment impedances it comprises

- a master robot with dynamics $z_{cm}(s)$, and local force and position gains $c_6(s)$ and $c_8(s)$,

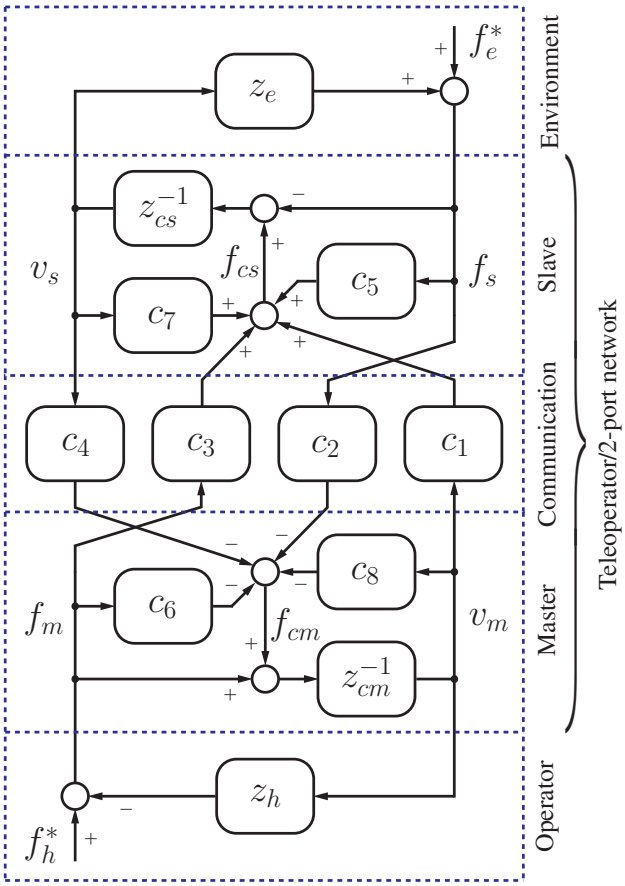

Figure 3.6: The Extended Lawrence Architecture (ELA).

- a slave robot with dynamics $z_{cs}(s)$, and local force and position gains $c_5(s)$ and $c_7(s)$, and
- a communication layer with gains $c_1(s)$–$c_4(s)$.

Also, f_{cm} and f_{cs} are the control output forces sent to master and slave motors, respectively. The term 'controller' is used to refer to a particular choice of values for the whole set of controller gains c_1–c_8. The performance analysis of a particular choice of controller involves an evaluation of the teleoperator's stability and telepresence properties; two complementary measures that trade off one another. Stability can be evaluated via, for example, passivity theory [26], singular value conditions [96] or absolute stability [97, 98]. The teleoperator's telepresence properties describe to what extent the operator feels present at the remote site, and it is evaluated by seeing how well the master force f_m and velocity v_m match their respective quantities f_s and v_s on the slave side [99, 55]. A transparent teleoperator will make sure that $f_m = f_s$ and $v_m = v_s$ at all times. Telepresence may also be substituted for other measures of fidelity, such as optimal sensitivity [57].

3.2.2 Global Teleoperator Transparency Analysis (Paper IV)

Since its introduction the Lawrence/ELA architecture has been used extensively in the analysis of both the stability and telepresence properties of various Class I teleoperation control designs [23, 100, 55, 101, 56]. However, transparency has always been shown 'by demonstration'. Certain choices of the controller gains c_1–c_8 have been shown to be a *sufficient* condition for transparency. For example, Lawrence [29] illustrated how choosing specific values for the communication layer gains c_1–c_4 is sufficient for transparency. Yokokohji and Yoshikawa [30] also reported of a teleoperation controller that achieved transparency by utilizing all four communication channels, roughly at the same time as Lawrence, but independently, thus reinforcing the belief that four channels were needed for transparency. Hashtrudi-Zaad and Salcudean [95] utilized the local force feedback gains c_5 and c_6 to achieve transparency with only three non-zero communication layer gains. Again, it was a demonstration of sufficiency. Kim et al. [102] showed that transparency may actually be achieved with only two non-zero communication layer gains. Fite et al. [103] also discussed the possibility of transparency with two channels.

Neither of the above-mentioned papers showed that their specific choice of gains was a *necessary* condition for transparency. Paper IV undertakes a global transparency analysis of the ELA in Figure 3.6. It states necessary *and* sufficient conditions for transparency for all Class I bilateral teleoperation controllers. Subsequent conditions are then derived that show how transparency can be achieved with only two non-zero communication layer gains. Transparency (telepresence) is the exclusive topic of Paper IV. Stability is an equally important aspect of teleoperation controller design, and while it is fine to consider telepresence and stability separately in an earlier design phase, the two must eventually be studied together. Paper IV may also be considered an introduction to the kind of 2-port network analysis that is used to develop the concept of *Force Sensor Free* (FSF) teleoperation in Paper V.

3.2.3 Interaction Force Estimation in Teleoperation (Paper V)

Controllers for bilateral teleoperation that aim to achieve a maximum degree of telepresence most often make use of interaction force measurements. It seems logical that in order to implement realistic force feedback, information about these forces must be communicated within the system in one way or another. Due to the difficulties associated with incorporating force sensors in a teleoperation system (and particularly in teleoperated keyhole surgery), numerous efforts have been made to obtain the interaction forces by *estimation* rather than by measurement. In general, estimation of a quantity that is not measurable is done by utilizing information about one or more quantities that *are* measurable. For the purpose of interaction force estimation in teleoperation, that information may be obtained internally from within the teleoperation system, or externally from the connecting entities (human operator, environment, or both). In the former case the measurable quantities may be the state of the robots, the motor forces (torques) and the dynamic parameters of the robots [104, 105, 106, 107]. In the latter case the mea-

surable quantities may be the dynamic parameters of the operator and environment, and their respective motion variables, measured for example by vision systems [108, 109]. Only internal information-driven estimation is considered here.

Paper V studies the effect on performance caused by the estimation of the master and slave interaction forces. The main message is that the estimation of the two forces f_m and f_s must be viewed as one problem. The reason is that the two forces are functions of each other; applying one force will have an effect on the other force. By writing out the dynamics of a Class II teleoperator on the general form

$$\boldsymbol{Q}\boldsymbol{f} + \boldsymbol{R}(\boldsymbol{v}) = \boldsymbol{0} \tag{3.5}$$

where $\boldsymbol{f} := [f_m, f_s]^T$, $\boldsymbol{v} := [v_m, -v_s]^T$ and the linear matrix $\boldsymbol{Q}$ and the nonlinear vector $\boldsymbol{R}$ reflect the contents of the 'Teleoperator' block in Figure 3.5, the problem of estimating f_m and f_s becomes one of solving the matrix equation (3.5) with respect to $\boldsymbol{f}$. Whenever $\boldsymbol{Q}$ is singular, a solution does not exist, and interaction forces cannot be estimated. For Class I teleoperators Paper V also introduces the notion of *equivalent controllers*, and it is shown how that can be utilized to establish the Force Sensor Free (FSF) transformation. The FSF transformation accepts a general Class I ELA controller (a set of controller gains c_1–c_8) and outputs a new ELA controller with identical stability and telepresence characteristics, but where force measurements are not utilized. The output of the FSF transformation is referred to as an FSF controller. The FSF transformation is an aid in the effort to understand the theoretical effect of force estimation within the familiar framework of the ELA controller, but it is also a procedure that allows controller design to be done assuming that force measurements are available, even when they are not.

The experiments in Paper V focus on the validation of the FSF transformation. The purpose of the experiments is to compare the stability and telepresence properties of two teleoperation controllers; some given ELA controller that relies on interaction force measurements and the FSF-transformed version of that same controller. The comparison is done using both raw data and fitted data. Raw data are compared by plotting the force and position profiles as a function of time for the two teleoperation systems while touching a sample gel that mimics human tissue. Fitted data are compared via an empirical calculation of the hybrid matrix representation of the two teleoperation systems [110]. The laboratory setup is a custom-built teleoperation system using two PHANTOM Premium haptic devices (Sensable Technologies, MA, USA) and a PXI embedded controller (National Instruments, TX, USA). The reader may consult Appendix A for the details on that system.

3.3 Force Sensor Free Teleoperated Robotic Surgery

The focus of this thesis is to develop new methods for realistic or task-optimized force feedback in teleoperated robotic surgery. To that end, research objectives 1 and 2 presented in Sections

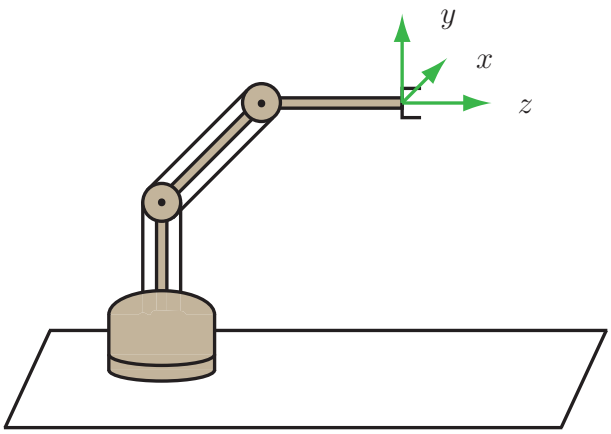

Figure 3.7: Serial-link robot with workspace coordinates.

3.1 and 3.2, respectively, are independent efforts that must be brought together in order to realize a teleoperation system that is capable of delivering the sought-after objective 3; force sensor free teleoperated surgery with task-optimized force feedback. Section 3.3.1 utilizes the friction estimation and parameter identification of Section 3.1 to enable the linear 1-DoF interaction force estimation schemes of Section 3.2 to be implemented on nonlinear multi-DoF real robots. Section 3.3.2 then goes one step further to develop a *2-stage sensitivity-optimized control scheme tailored for soft-tissue surgery*.

3.3.1 Real-World Application of Linear 1-DoF Theory

The dual force estimation theory of Section 3.2 is only valid for 1-dimensional teleoperators. Furthermore, the Force Sensor Free (FSF) transformation assumes the system is linear. However, robots are in most cases multi-dimensional and nonlinear. Hence, in order to implement design schemes based on what was developed in Section 3.2, the dynamics of the master and slave robots must be decoupled and linearized.

Consider the serial-link robot in Figure 3.7. It is the same robot as in Figure 3.1, except that workspace coordinates are shown instead of joint-space coordinates. Recall that the robot's dynamic equation in joint-space is given as

$$\boldsymbol{M}(\boldsymbol{q})\ddot{\boldsymbol{q}} + \boldsymbol{C}(\boldsymbol{q},\dot{\boldsymbol{q}})\dot{\boldsymbol{q}} + \boldsymbol{N}(\boldsymbol{q}) + \boldsymbol{\tau}_f = \boldsymbol{\tau}_c + \boldsymbol{\tau}_s. \tag{3.6}$$

The strategy is to change the *apparent* dynamic behavior of the robot into

$$\boldsymbol{M}_w\ddot{\boldsymbol{p}} = \boldsymbol{F}_c + \boldsymbol{F}_s \tag{3.7}$$

where $\boldsymbol{M}_w := \text{diag}(m_x, m_y, m_z) \in \mathbb{R}^{3\times3}$ is a chosen mass matrix, $\boldsymbol{p} := [x, y, z]^T$ is the posi-

tion of the end effector relative to the base of the robot, $\boldsymbol{F}_c$ is the effective control output force and $\boldsymbol{F}_s$ is the interaction force. Eq. (3.7) represents three linear, independent 1-DoF point mass systems. The transition from the joint-space equation (3.6) to the workspace equation (3.7) takes place by applying a torque to the joints of the robot that effectively decouples its dynamic behavior. Such decoupling of the robot's dynamics is usually referred to as a *computed-torque method* [111], which is a well-known method, and not a contribution of this thesis. However, the computed-torque method relies on the knowledge of $\boldsymbol{M}$, $\boldsymbol{C}$, $\boldsymbol{N}$ and $\boldsymbol{\tau}_f$. That is where the friction estimation and parameter identification methods of Section 3.1 come into play, because their accuracy will have a direct impact on the accuracy of the computed-torque method. With the dynamics of the master and slave robots decoupled, the FSF transformation may be implemented on a per workspace axis basis.

3.3.2 Task-Optimized Robotic Surgery (Papers VI and VII)

Çavuşoğlu et al. [57] argued that the design of a bilateral teleoperation controller should be specific to the task at hand, that is, the controller should be task-optimized. It is not obvious that telepresence, the traditional performance metric, represents the optimum type of performance for all types of tasks. In surgery a common task is the manipulation of soft tissue. For this task the teleoperator should have the ability to convey the smallest possible changes in tissue compliance to the surgeon. Thus, sensitivity should perhaps be pursued rather than transparency. As part of the analysis in [57] it was also demonstrated that obtainable sensitivity increases if interaction force measurements are available. Because it is difficult to mount force sensors on the small surgical instruments of the slave robot, sensitivity is in danger of being compromised. To battle that threat, we propose a 2-stage controller design method that

I. designs a *Sensitivity-Optimized* (SO) Class I bilateral teleoperation controller based on a modified version of the methodology of [57], and

II. applies the FSF transformation to the controller of Stage I in order to create a *Sensitivity-Optimized Force Sensor Free* (SOFSF) controller that is specifically aimed at teleoperated robotic surgery.

Stage I of the controller design consists of formulating and solving a constrained optimization problem with respect to the controller gains c_1–c_8 of the ELA in Figure 3.6. The cost function is a measure of the teleoperator's sensitivity, and there are three constraints that must be observed; a tracking constraint, a stability constraint and an FSF existence constraint. The tracking constraint is necessary to avoid trivial solutions to the optimization problem. The stability constraint is necessary in order to guarantee the robustness of the system. The stability constraint in [57] requires known bounds on both the environment impedance z_e and the human operator impedance z_h (see the 2-port network in Figure 3.5), of which the latter is particularly hard to determine, as the dynamics of a human operator are highly nonlinear and time-varying.

Instead, the 2-stage method uses the stability constraint introduced by Haddadi and Hashtrudi-Zaad [28], which only requires known bounds on the environment impedance. Finally, the FSF existence constraint is necessary in order to prevent that the solution to the optimization problem yields a poorly conditioned $\boldsymbol{Q}$ matrix in (3.5). The FSF existence constraint guarantees a well-defined FSF transformation in Stage II. The choice of controller parameters is a generalization of the original formulation in [57], as the size of the parameter space is extended from 2-dimensional to 8-dimensional.

The 2-stage teleoperation controller design method is tested in two ways. First, an approximate sensitivity value σ are calculated and compared for the SO and SOFSF controllers through an automated palpation task in Paper VI. The teleoperation system automatically palpates a tissue gel that contains a metal bolt inserted underneath its surface. The metal bolt produces a change in impedance, and the calculated sensitivity value measures how well that change is conveyed from slave to master side. Appendix A explains how the automation is realized. Second, Paper VII presents the results of a human perception test; the human-operated equivalent of the automated palpation task of Paper VI. A number of human subjects are asked to locate the metal bolt underneath the surface of the gel, using the teleoperation system, and without being able to see the slave and the gel. The idea is to use statistical methods to evaluate and compare the sensitivity of the SO and SOFSF controllers. Appendix A explains how the test equipment is set up, and the test procedure is found in Paper VII.

Chapter 4

Summary of Results

This chapter provides a brief summary of the results achieved in each of the original papers; as a theoretical result, an experimental result, or a combination of the two.

4.1 Single Estimation Force Estimation

4.1.1 Estimation of Coupled Friction (Paper I)

Purpose/Contribution of paper To show that an expansion/network of wavelets has a better ability to estimate friction than a simple Coulomb+viscous friction model in a robot where friction may be coupled between multiple joints, typically caused by a cable transmission.

Outcome During training of the wavelet network the relative *Root-Mean-Square* (RMS) motor torque estimation errors were reduced by up to 30.5% compared to the Coulomb+viscous model[1]. However, during validation of the wavelet network, performance was worse than for the Coulomb+viscous model, manifested by increased motor torque estimation errors, and it highlighted the need to improve the way the wavelet network was trained.

4.1.2 Parameter Identification by Manual Excitation (Paper II)

Purpose/Contribution of paper To show that manual excitation of the robot during the collection of training data will improve interaction force estimation performance compared to using conventional motor torque excitation (as in Paper I).

Outcome Manual excitation resulted in a reduction of the relative RMS estimation errors ranging from 21% to 35% between the three joints of the Omni compared to motor torque excitation. It was also observed how the manual excitation algorithm adjusted the motor torque constants to presumably more correct values. Presumably, because the actual motor constants

[1] In Paper I, estimation error reductions are quoted in *percentage points* (pp).

were unknown, but the adjustments resulted in improved interaction force performance. Finally, the richness of the training data was seen to be much higher than with motor torque excitation, thus resulting in improved training of the wavelet network friction model.

4.1.3 Estimation in Robots with Elastic Cables (Paper III)

Purpose/Contribution of paper To employ an Unscented Kalman Filter (UKF) for state and parameter estimation in an elastic transmission, and study its robustness to unknown variations in inertia, cable tension and interaction forces.

Outcome The UKF successfully estimated the unknown parameters of the elastic transmission, and also the motor and link angles and velocities under nominal conditions. Although the transmission was very stiff, and hence the motor and link states almost identical, information about the individual quantities was obtained. When varying the inertia of the link, state estimation performance stayed almost constant until the inertia reached about 2.5 times its nominal value, after which the estimation performance deteriorated quickly. The most interesting phenomenon that was observed when varying the tension of the cable was that estimation performance seemed to stay constant or even improve as cable tension decreased (which it is bound to do over time). There was a near-linear relationship between increasing interaction forces and state estimation errors, suggesting that interaction forces might be estimated using this error information, at least in a steady-state sense. Irrespective of variation from nominal conditions, using the UKF link angle estimate was better than using motor angle as an approximation (that is, an inelastic transmission assumption). The same was not true for the velocity estimate. Overall, the angle estimates were particularly robust to variation in operating conditions, and more so than the velocity estimates.

4.2 Dual Interaction Force Estimation

4.2.1 Global Teleoperator Transparency Analysis (Paper IV)

Purpose/Contribution of paper To formally analyze the global transparency characteristics of the Extended Lawrence teleoperator Architecture (ELA).

Outcome The analysis may be regarded as theoretical groundwork for Papers V, VI and VII, but also as a stand-alone effort. The results consisted of a transparency theorem with two accompanying corollaries, plus a demonstration of redundancy in the original Lawrence architecture. The theorem stated the general solution to the problem of achieving transparency in bilateral teleoperation. It was shown that there is an infinite number of solutions that all yield transparency. The first corollary gave a condition on the relationship between the communication

layer gains c_1–c_4 of the extended Lawrence architecture that must be satisfied for transparency to be possible. The second corollary formally showed how transparency can be achieved using only two of the gains c_1–c_4 in the communication layer. The purpose of the redundancy demonstration was to illustrate how a communication layer gain in the original Lawrence architecture can in some cases be replaced by a local gain, while preserving transparency. Hence, the communication layer gain is redundant.

4.2.2 Interaction Force Estimation in Teleoperation (Paper V)

Purpose/Contribution of paper To study the effect of interaction force estimation on performance in bilateral teleoperation, and introduce the Force Sensor Free (FSF) transformation.

Outcome The main result of the first part of Paper V was a proposition that points out the existence of a singularity in a teleoperation system, close to which interaction force estimation becomes infeasible. The potential singularity of the matrix $\boldsymbol{Q}$ in (3.5) serves as evidence that the achievable performance in teleoperation is limited in the absence of force sensors. A case study showed that when $\boldsymbol{Q}$ is poorly conditioned (near-singular), interaction force estimation becomes infeasible in practice, due to closed-loop feedback gains that approach infinity. Thus, the system becomes vulnerable to aspects not accounted for, such as phase lag from low-pass filtering during practical implementation.

The second part of Paper V was dedicated to the development and validation of the FSF transformation. Validation was done through an experimental comparison of a sample teleoperation controller and its FSF-transformed counterpart. In theory, these controllers are equivalent. When comparing force and position profiles, the two controllers did perform very similarly during contact with the gel. However, during free-space motion, the FSF controller performed worse than the original controller. The master force of the FSF controller was of a fluctuating character, while it stayed close to zero for the original controller, which is what it should do when the slave is not touching the gel. When comparing the elements of the hybrid matrices of the two controllers, it was found that their frequency responses were almost identical in the lower frequency segment, which is logical, since that is where the data were recorded. For higher frequencies the responses did not match as well.

4.3 Force Sensor Free Teleoperated Robotic Surgery

4.3.1 Task-Optimized Teleoperation Controller (Paper VI)

Purpose/Contribution of paper To obtain realistic, sensitivity-optimized force feedback tailored for use in teleoperated robotic surgery, with the use of a 2-stage controller design method that merges sensitivity optimization and interaction force estimation.

Outcome The automated palpation experiment resulted in average approximate sensitivity values of $\sigma = 0.285$ for the Sensitivity-Optimized (SO) controller of Stage I and $\sigma = 0.202$ for the Sensitivity-Optimized Force Sensor Free (SOFSF) controller of Stage II. In comparison, the predicted sensitivity — the outcome of the optimization problem in Section 3.3.2 and denoted by σ_c — was computed to be $\sigma_c = 0.211$. A Mann-Whitney statistical test determined that the sensitivity of the SOFSF controller was significantly lower than that of the SO controller on the 5% level, with a p-value of $p = 0.00002$.

4.3.2 Evaluation through Human Perception Test (Paper VII)

Purpose/Contribution of paper To show that the SO and SOFSF controllers of the 2-stage design method have identical sensitivity characteristics through a perception test with human participants and statistical analysis.

Outcome The sensitivity of the SO and SOFSF controllers were determined based on their ability to help the human operator locate the metal bolt in the tissue gel (shown in Figure A.4(a)). In theory, the more sensitive controllers should be better at locating the bolts. The hypothesis behind the design of the test was that the SO and SOFSF controllers would be equally sensitive, and statistically set apart from a benchmark controller whose theoretical sensitivity was lower. However, the results came out inconclusive. Hence, the outcome of Paper VII was instead a set of design aspects that will have to be addressed and improved upon before being able to observe differences in sensitivity.

Chapter 5

General Discussion

5.1 Single Interaction Force Estimation

The literature contains a lot of work on the identification of the physical parameters of robots. However, less work can be found on cable-driven robots, particularly in terms of the identification of joint friction. The cable transmission system makes identifying friction parameters a difficult task. This part of the thesis therefore mainly focused on finding a simple friction model that was able to capture coupled friction phenomena.

Paper I presented the wavelet neural network as a possible solution to finding a simple friction model. It was chosen because it is mathematically simple and because no predetermined model structure is needed, but most importantly it was chosen because it may easily be extended to multiple dimensions. The latter makes the wavelet friction model suitable for the approximation of friction in a cable transmission, since multiple variables from different joints of the robot may be fed as input to the model. The results also indicated that the wavelet friction model performed better than a conventional Coulomb+viscous friction model. That is, it performed better during the training phase (when the model parameters are estimated). During the validation phase (when the model parameters are tested) the problem of achieving adequate training became evident. It was hard to provide the wavelet friction model with sufficiently general training data, hence performance was affected during validation.

Manual hand excitation of the robot was introduced in Paper II as a training technique with three distinct advantages; 1) as a random trajectory generator, manual excitation would provide training data with a high degree of richness, thereby mitigating the main problem of Paper I, 2) integrated dynamic estimation of the motor constants enables a more accurate adjustment of the data sheet figures and gear ratios, and 3) when the ultimate application is interaction force estimation, manual excitation training directly seeks to minimize the force estimation error. These advantages together resulted in an improvement of interaction force estimation performance of up to 35%, compared to using motor excitation. However, manual excitation comes with two main limitations. First, a force sensor must be attached to the tip of the robot

during the collection of training data. That may seem to defeat the purpose of avoiding the use of force sensors in the first place. The best option would be to build a force sensing adapter that can easily attach to and detach from the tip of the robot. The adapter can then function as an intermediate connection point between the hand of the operator and the robot during training, and then detach for normal operation. There will, however, be a slight change of dynamics, due to the weight and length of the adapter. The second limitation of manual excitation is that it requires the robot to be backdrivable. Lightweight, direct-drive robots such as the PHANTOM Omni are usually backdrivable, but heavier industrial robots with large gear ratios may not be.

Paper III should be set aside somewhat from the main path of the work, as interaction force estimation was only a secondary topic. Focus was primarily on the robustness of the state estimates in an elastic transmission under changing operating conditions. On the other hand, the ability of the inverse dynamics algorithm — the underlying principle of estimation in this thesis — to correctly estimate the interaction force will depend on the accuracy and *robustness* of the system parameters and state estimates. Hence, the robustness study of Paper III may be regarded as an indirect study of interaction force estimation ability under changing operating conditions. One such change was, interestingly, the application of an interaction force. It was found that a linearly increasing interaction force resulted in a near-linearly increasing state estimation error. That correlation can perhaps be exploited to obtain a simple estimate of the value of the force, but it was not studied further in this thesis.

In the pursuit of research objective 1, two aspects of interaction force estimation in cable-driven robots were treated; joint friction and cable elasticity. However, they were treated separately, one without the other. Papers I and II studied the use of wavelets for friction estimation, but the cables were assumed to be inelastic. Paper III studied state estimation in an elastic transmission with one Degree of Freedom (DoF), but no wavelet model was used for friction estimation. Ultimately the goal is to estimate $\boldsymbol{F}_s$ in Figure 2.1, that is, a multi-dimensional interaction force. In order to develop a complete interaction force estimation scheme for a multi-DoF cable-driven robot with elastic cables and coupled friction, the wavelet network friction model must be merged with the UKF algorithm. Building a UKF for a cable-driven robot with, say, 6 DoFs is a challenging task in itself, because of the large number of variables. The UKF must be extrapolated on a joint-by-joint basis, or a new UKF algorithm must be built around a complete model of a cable-driven robot with elasticity taken into account, such as the model in [112]. Still, the bigger challenge will perhaps be the adaptation of the wavelet coefficients, since there may be thousands of them, and it is not obvious how the adaptation should be done efficiently inside the UKF framework. The most likely solution is some sort of a parallel adaptation approach, where the state estimates from the UKF are continuously used in the adaptation of the wavelet coefficients, and vice versa.

5.2 Dual Interaction Force Estimation

When the two interaction forces (master and slave side) of a teleoperation system are estimated, they are commonly treated individually as two separate estimation problems. The central claim of research objective 2 was that they should be treated as one and the same problem.

Paper IV did not study interaction force estimation at all. Nevertheless, its formal discussion of transparency in linear teleoperation systems did contribute important knowledge, particularly about the flow of information throughout the system and between master and slave robots. One of the most important results was the realization that transparency is possible with only two channels of information being communicated between master and slave robots, such as velocity in one direction and force in the other. A potential criticism against Paper IV is that it dealt with transparency exclusively. Stability was ignored. However, studying one aspect of teleoperation does not mean that the other aspects have been forgotten. Paper IV was not intended as a complete recipe for teleoperation controller design. Rather, it was intended as a guideline for *transparent* controller design. The knowledge of the bilateral teleoperation system obtained in Paper IV also served as a good starting point for the work to be done in Paper V.

In general, the performance of any system that uses estimated interaction forces is limited compared to when force sensors are available, as a result of inaccurate estimation (due to imperfect knowledge of robot parameters, convergence time of force estimates etc.). The most important outcome of Paper V was the proof that the performance of a teleoperation system that uses estimated interaction forces is limited also on a theoretical level. That is, even if the interaction forces can be estimated with 100% accuracy, there is a performance limit, due to the existence of a singularity. Essentially, interaction force estimation in bilateral teleoperation is analogous to solving a set of two equations in two unknowns; there may not be a solution, or the solution might be poorly conditioned. The analysis of Paper V was general, encompassing nonlinear as well as linear systems. The only condition imposed was that the interaction forces appear linearly within the system. Hence, the analysis has a broad impact on the understanding of the governing mechanisms of interaction force estimation in bilateral teleoperation.

Paper V also introduced the Force Sensor Free (FSF) transformation for linear teleoperation systems, and a set of experiments was conducted in order to validate its operation. Closely linked performance was observed between the original controller and its FSF-transformed version, as predicted by theory. However, differences in performance were also observed, particularly at higher frequencies, demonstrating the inevitable effect of inaccurate force estimation. Several factors may explain inaccurate estimation. These include

- inadequate or insufficient modeling of the robots,
- inaccurate identification of the dynamic parameters of the PHANTOM Premiums, and
- low-pass filtering of force, velocity and acceleration.

A very good example that involves all of the above factors is the computed-torque method of Section 3.3.1. First, the computed-torque method relies on the dynamic equation correctly describing the actual behavior of the robot. In reality the dynamic equation that was used for the PHANTOM Premiums was a simplification. It did not model internal vibration modes created by the cable transmissions, structural flexibility or backlash. Second, the computed-torque method relies on the parameter identification being accurate. As seen from the results in Papers I and II, the wavelet network friction model did not achieve perfect results. In other words, the parameter estimation was accurate only to a certain extent. Finally, the joint angles, velocities and accelerations were not known exactly. Optical encoders with a finite resolution were used for angle measurement, and both velocity and acceleration were passed through low-pass filters, resulting in poor approximations at higher frequencies.

More than anything, the outcome of the pursuing of research objective 2 was an increased understanding of the basic workings of a bilateral teleoperation system, and the effect that estimating the interaction forces will have on the performance of that system. The most important result was the fact that there exists an interaction force estimation singularity in a bilateral teleoperation system. Any controller design that aims to estimate the interaction forces must maintain a safe distance (quantified using some measure of closeness) to that singularity, in order to preserve a robustly stable system. The shorter the distance, the better the telepresence. It is the classic stability-telepresence trade-off over again. What makes a 'safe distance' is determined by the quality of the particular hardware (robots) in use. High quality hardware allows a shorter distance to the singularity. A highly interesting research topic would be a systematic robustness analysis that determines/quantifies the safe distance for a given teleoperation system, and, once it is found, looks for the most economic ways to make it shorter. For example, what is more important, accurate friction estimation or accurate acceleration measurement?

5.3 Force Sensor Free Teleoperated Robotic Surgery

Research objective 3 brought objectives 1 and 2 together in a logical sequence of research efforts, moving forward from the development of algorithms with a large range of applications towards the specific integration of these algorithms for use in force sensor free teleoperated robotic surgery. The product was the 2-stage controller design method for sensitivity-optimized teleoperation without force sensors, addressed in Papers VI and VII.

The sensitivity σ of a transparent teleoperation system is unity, since all actions on the slave side are always communicated to the master side in their exact form. Thus, one would expect that a teleoperation system that implements a control scheme particularly developed to maximize sensitivity would have a sensitivity value $\sigma \geq 1$. In Paper VI, the output of the optimization routine of the 2-stage method was computed to be $\sigma_c = 0.211$. In the automated palpation experiment, the average measured sensitivities of the Sensitivity-Optimized (SO) controller of Stage I and the Sensitivity-Optimized Force Sensor Free (SOFSF) controller of Stage

II were measured at $\sigma = 0.285$ and $\sigma = 0.202$, respectively. Hence, there was good accordance between predicted sensitivity σ_c and measured sensitivities σ for both controllers. However, the attained sensitivity of the 2-stage design method was lower than expected. One important reason is the fact that the solution to the optimization problem was conservative, due to the existence of the constraints. Maintaining system stability and the well-definedness of the FSF transformation reduces the attainable sensitivity. Furthermore, a transparent teleoperator is not realizable either, because it is only marginally stable. Hence, the direct comparison of numbers is unfair. The difference in measured sensitivity, $\sigma = 0.285$ for the SO controller versus $\sigma = 0.202$ for the SOFSF controller, was determined to be statistically significant by a Mann-Whitney test. Consequently, inaccurate estimation of the interaction forces caused an additional loss of sensitivity, on top of the reduction in sensitivity induced by the estimation constraint in the optimization problem. The sources of inaccurate force estimation remain the same as discussed in the previous section for Paper V. With respect to sensitivity, the low-pass filtering of signals that are used in the estimation (particularly velocity and acceleration) is perhaps particularly important, since a low-pass filtered signal has a decreased ability to change quickly.

The experiment of Paper VI was an objective test of the 2-stage design method, since it was without human influence. The goal of Paper VII was to evaluate the 2-stage method through a subjective perception test involving human operators. Their task was to palpate the tissue gel using the teleoperation system with a controller (SO, SOFSF or benchmark), but they also palpated the gel manually using a pen. In that sense the 2-stage method could be compared against the 'golden standard' of manual palpation. As mentioned in Section 4.3.2 the test results were inconclusive, due to inadequate test design. However, the results did indicate that manual palpation was superior to teleoperated palpation, regardless of whether the SO or SOFSF controller was used. In that sense, Paper VII confirmed the results of Paper VI, since manual palpation is 'transparent' palpation ($\sigma = 1$) and the measured sensitivities of the SO and SOFSF controllers in Paper VI were lower than 1. Ideally, it would be desirable to exploit the teleoperation system to enhance sensitivity beyond the natural abilities of the surgeon ($\sigma > 1$). That is possible [17], but the challenge is preservation of stability. The system must remain robust to inaccuracies and disturbances.

In view of the inconclusive results of Paper VII, is it fair to say that research objective 3 was accomplished? In terms of *developing* a method for 'force sensor free teleoperated robotic surgery with realistic or task-optimized force feedback' as stated in section 2.2, research objective 3 was accomplished through the 2-stage design method. In terms of *testing* the same method, research objective 3 must be said to be only partly accomplished. A successful user-centered or surgeon-centered perception test like the one in Paper VII would add credibility to the 2-stage design method, because it would validate the method's properties with statistical methods, and because the setup of the test directly reflects a real palpation task (with a human operator involved in the task).

5.4 In a Greater Context

In the 2-stage teleoperation controller design method of Papers VI and VII, Stage I consisted of a Sensitivity Optimization (SO) control scheme, particularly aimed at robotic surgery and the manipulation of soft tissue. It would be straightforward to substitute the SO scheme with any other control scheme, as long as the end product of Stage I is a linear system. One example is the affine enhanced stiffness perception method of De Gersem et al. [17]. Alternately, at the other extreme there are robust control schemes designed for the stable manipulation of hard/stiff environments, such as bone structures [27, 113]. It would even be possible to use control schemes with time-varying properties, since the whole 2-stage design method may in theory be executed at every time step during operation. The only requirement of the selected control scheme in Stage I — aside from being linear — is that it cannot violate the interaction force estimation singularity pointed out in Paper V. It is useful to note that the estimation singularity is also valid for nonlinear systems, although the FSF transformation of Stage II would have to be modified for the nonlinear version of the 2-stage controller design method.

All algorithms developed in this thesis as part of the effort to accomplish the three research objectives have been tested on real hardware. Real results from experiments have more value than theoretical results. Nevertheless, experimental testing of an algorithm may still be described as more or less realistic with regard to the final application of that algorithm. The final application of the algorithms developed in this thesis is teleoperated robotic surgery, whose circumstances differ in several ways from the laboratory test setup used in Papers V, VI and VII, and described in Appendix A. First, the PHANTOM Premium robot only have three actuated DoFs, and only translational motion and interaction forces (no torques) were considered in the experiments. Robots designed for teleoperated surgery, such as the daVinci system, have six or more DoFs with wrist-like end-effectors for increased dexterity inside the patient in keyhole surgery. Rotational motion is common, and the estimation of interaction torques (in addition to forces) is therefore essential for the improved applicability of the results. Second, robots intended for keyhole surgery must have thin and long links in order to reach inside the patient. Thus, the links may perhaps not be considered as absolutely rigid, and that will have to be taken into account during modeling and parameter identification. Thin links will also require small pulleys for the cable transmissions, thus increasing friction. That will put the wavelet network friction model to the test. Finally, the incision point — where the robot enters the patient — is another disturbance not accounted for in this thesis. It represents a kinematic constraint and a source of friction. However, by proper modeling of the incision point it is possible that the friction occurring there may be captured by the wavelet model.

Chapter 6

Conclusions

The following concludes the work presented in this thesis:

- A wavelet neural network friction model outperforms the common Coulomb+viscous friction model for cable-driven robots with complex friction features, while maintaining the same mathematical simplicity.
- A wavelet neural network friction model is highly dependent on adequate training in order to reach its full potential.
- In terms of collecting data to identify the dynamic parameters of a robot, manual excitation improves identification performance compared to automatic excitation (using only the motors of the robot).
- The Unscented Kalman Filter is suitable for full state estimation in an elastic transmission (both near and far states) where only motor (near) angle is measured, and where nonlinear elasticity is taken into account in the dynamic model.
- The position estimates of the Unscented Kalman Filter are robust to variations in operating conditions (such as changing cable tension), while the velocity estimates are less robust. A near-linear relationship between applied interaction force and state estimation error may be exploited to obtain a simple estimate of the value of the interaction force.
- Transparency in bilateral teleoperation is possible with only two channels of information being communicated between master and slave robots, one channel in each direction. The channels must carry complementary information (force and velocity).
- The Lawrence teleoperator architecture is redundant. Hence, there is an infinite number of controllers that yield transparency.
- There is a singularity inherent to every bilateral teleoperation system, at which interaction force estimation is theoretically impossible, and close to which it is practically infeasible.

- The Force Sensor Free (FSF) transformation exploits algebraic properties of a linear teleoperator to turn a general controller (that uses interaction force measurements) into an FSF controller with identical stability and telepresence properties.
- While the original controller and its FSF-transformed version are *theoretically* equivalent, their *experimental* equivalence will — like with any other force estimation scheme — depend on the level of detail in the modeling of the hardware, the accuracy of the parameter identification, and the general quality of the hardware.
- The 2-stage controller design method attains the highest possible sensitivity of a teleoperation system when interaction forces are estimated.
- It is difficult to attain a sensitivity that is not lower than that of direct manipulation. Optimization constraints that guarantee stability and well-behaving interaction force estimates reduce the attainable sensitivity.
- Low-pass filtering of signals that are used to estimate interaction forces (particularly velocity and acceleration) will adversely affect the teleoperator's sensitivity.
- With respect to the objectives of Section 2.2, a complete scheme for force sensor free robotic surgery with task-optimized force feedback has been developed in this thesis. Further testing in a more realistic setting, closer to clinical application, is necessary to study the full potential of the scheme.

In Chapter 1, the lack of haptic feedback is mentioned as one of the factors that impede widespread use of teleoperated robotic surgery, much because of the difficulties associated with the use of force sensors in combination with small surgical instruments. The research objectives of Chapter 2 are formulated as a recipe that will restore the sense of touch to the surgeon, via the use of interaction force estimation. The answers given in this thesis — the methodologies, the theoretical and experimental results — describe the potential, but equally the limitations, of the use of estimated interaction forces in bilateral teleoperation in general, and in teleoperated robotic surgery in particular. They lay down the technical foundation for force sensor free surgery with real robotic surgical systems, such as the daVinci. If realistic haptic feedback through the use of interaction force estimation becomes a reality in teleoperated robotic surgery, it will lead the way to systems that have a performance superior to what exists today, and that are financially more attractive, and mechanically and technically less complex than systems that rely on the use of force sensors.

Appendix A

A Custom-Built Teleoperation System

All bilateral teleoperation experiments in this thesis were conducted using a custom-built setup and an in-house developed control system. The setup, shown in Figure A.1, consists of two identical PHANTOM Premium 1.5 haptic devices (SensAble Technologies, MA, USA), both with 6-DoF force/torque sensors mounted on the tip. The master force sensor is a Nano25, and the slave force sensor is a Nano17 (both ATI Industrial Automation, NC, USA). The control system for the two Premiums was developed using the LabVIEW 2009 software suite and the LabVIEW Real-Time Module with the PXI-8195 embedded controller (National Instruments, TX, USA). The user interface resides on a host computer running Windows Vista, and it communicates with the PXI-8195 via Ethernet. For some of the experiments human tissue was imitated with a polyvinyl alcohol (PVA) gel. It is made by dissolving the PVA in hot water at a certain weight percentage, and repeated freeze-thaw cycles determine the stiffness of the gel.

Figure A.2 illustrates the architecture of the control system. At the bottom can be seen the two robots and their force sensors. The force/torque signals from the force sensors are read by a PXI-6229 I/O board and sent directly to the PXI-8195. The encoder signals from the robots are sent to a PXI-7833R I/O board with an on-board 40MHz FPGA chip. The encoder signals are used in two ways; by a quadrature encoder to compute the angle of the robot's joints, and by an intelligent velocity estimation algorithm to compute joint velocity [114]. Joint acceleration is estimated by a low-pass filtered first difference approximation. The joint angles, velocities and accelerations are then sent to the PXI-8195. Motor torque commands are sent in the other direction. The PXI-8195 contains two loops; the core control loop executing at 1kHz with high deterministic reliability, and a 'slow loop' executing at 100Hz for data logging. The slow loop also communicates non-critical information, such as the continuous updating of the status of the robots (angles, velocities, forces etc.) from the controller to the user interface on the host computer, and the sending of higher level user commands from the user interface to the controller (start, stop, pause etc.). The physical separation of the control loop and the user interface allows the embedded controller to focus entirely on time-critical tasks, while the host computer takes care of the more time-expensive information to and from the user.

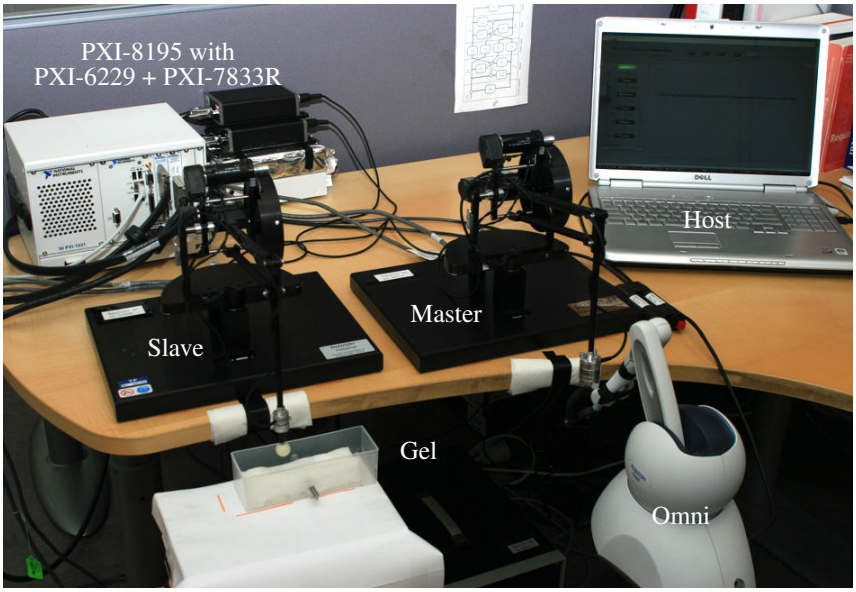

Figure A.1: Experimental setup for bilateral teleoperation, hardware components.

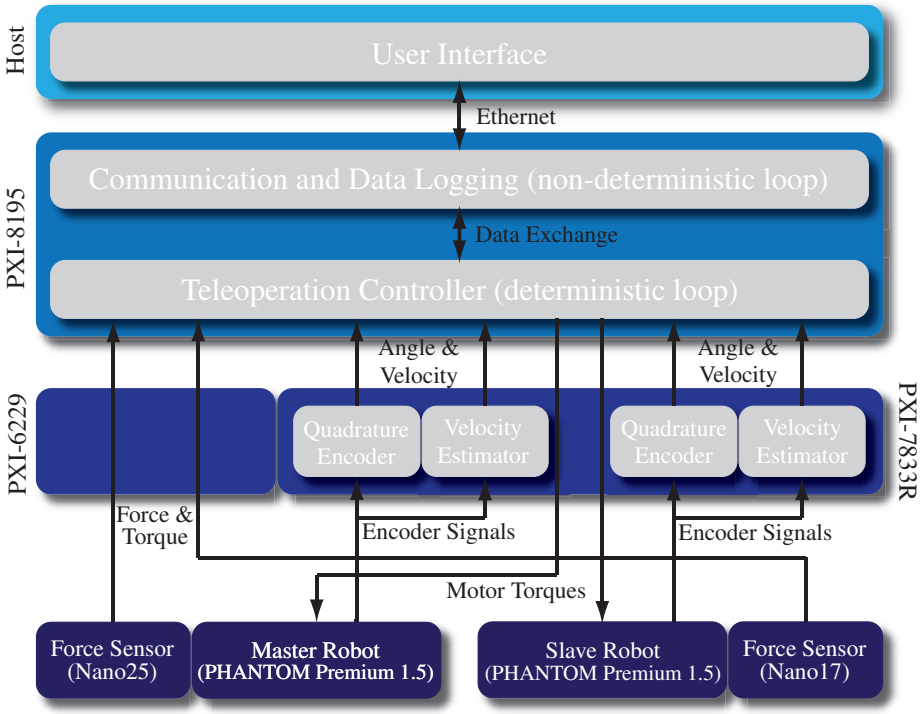

Figure A.2: Experimental setup for bilateral teleoperation, system architecture.

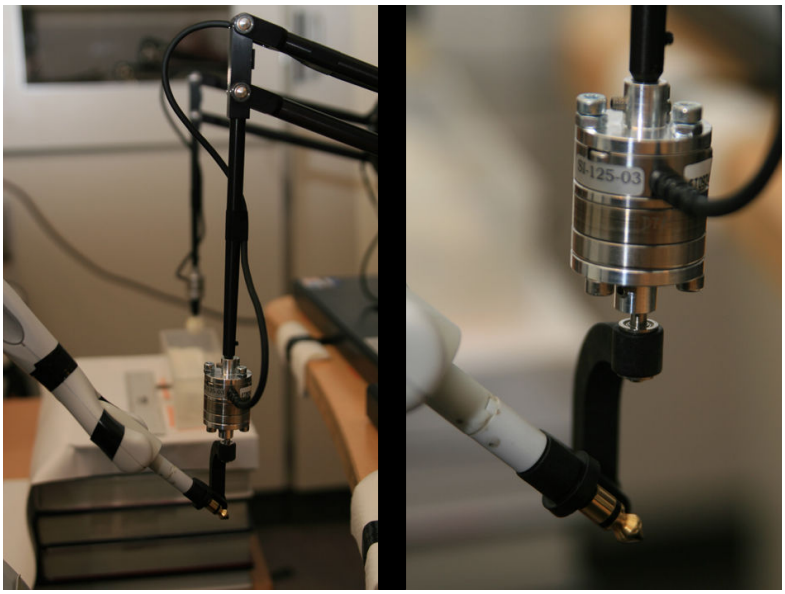

Figure A.3: The Omni-to-master attachment mechanism.

In order to record the data for the plotting of the force and position profiles in Paper V in an objective and repeatable way, the human operator was replaced by a PHANTOM Omni robot operator, after the idea of Conti and Khatib [115]. The Omni was programmed to move up and down in a sinusoidal fashion while the tip of the slave robot was intermittently touching the tissue gel. The Omni operator can be seen in Figure A.1, and a close-up of the attachment mechanism is shown in Figure A.3. Using a mechanical operator allowed for an objective excitation of the teleoperation system, and the execution of a sinusoidal trajectory could be repeated as many times as needed for the comparison of the two controllers. The automated palpation experiment in Paper VI also used the same setup. The Omni was programmed to palpate the tissue gel at a certain speed, pushing down into the gel with a certain downward force. The gel now contained a metal bolt inserted underneath its surface, resulting in a change of impedance as the tip of the slave robot crossed over the bolt. An approximate sensitivity value was calculated, which measured how well the change of impedance was conveyed from slave to master side.

The human perception test in Paper VII used the same core custom-built teleoperation system as in Papers V and VI, but with some important modifications and extensions. For practical reasons, only the slave robot had a force sensor, the Nano17. Figures A.4(a) and A.4(b) show the master and slave setup of the perception test. The two sides were visually separated, so that the operator was not able to see the slave side setup. As a replacement for the lack of visual contact with the slave, a gel visualization board was put in place underneath the handle of the master robot. In that way the test subjects could always see where the tip of the slave was lo-

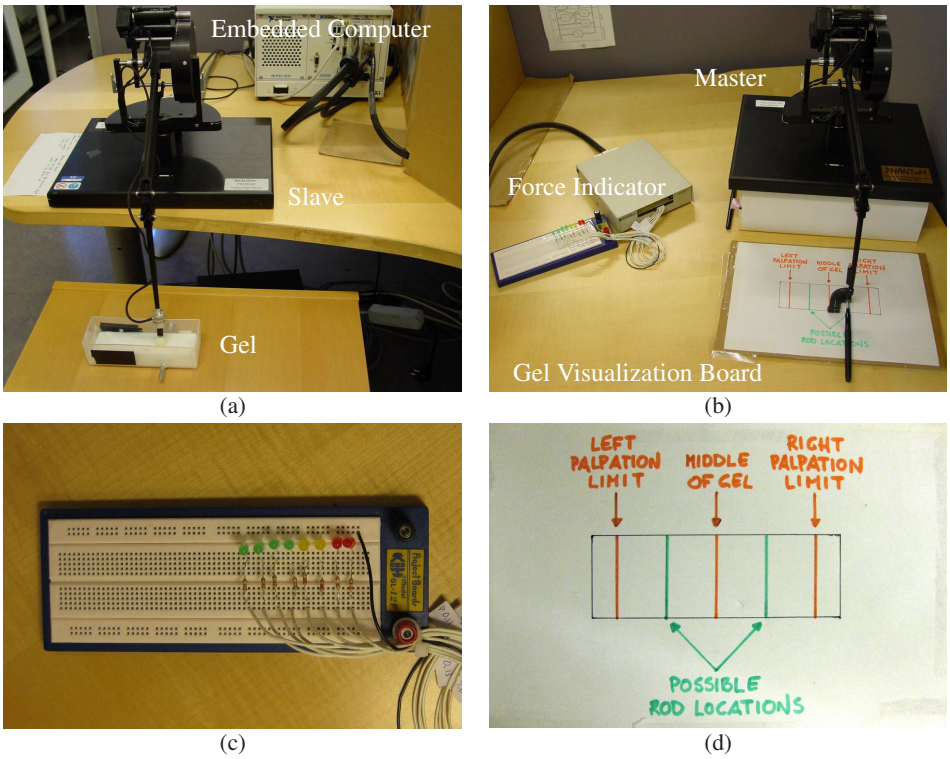

(a) (b)

(c) (d)

Figure A.4: Setup for human perception test. (a) Slave side (obstructed from the view of the subject), (b) master side with force indicator and gel visualization board, (c) Force indicator to prevent excessive forces and overheated motors, and (d) gel visualization board to guide the operator during palpation.

cated on the gel surface at all times. A force indicator with green, yellow and red LED lamps was provided to protect the Nano17 force sensor on the slave from overloading, and to prevent the overheating of the Premium motors. Furthermore, it also ensured that all the subjects applied forces of similar magnitudes. The PVA concentration of the gels was 6% by weight. Two freeze-thaw cycles were used to get the desired gel consistency. The appropriate gel concentration was determined by presenting gels with different concentrations to a laparoscopic surgeon at the Intervention Centre, looking to achieve a consistency similar to a human liver.

Appendix B

Original Papers

Paper I

Citation:
E. Naerum, J. Cornellà and O.J. Elle, "Wavelet networks for estimation of coupled friction in robotic manipulators", in *Proc. IEEE Conference on Robotics and Automation*, Pasadena, CA, USA, May 2008, pp. 862-867.

Paper II

Citation:
E. Naerum, J. Cornellà and O.J. Elle, “Contact force estimation for backdrivable robotic manipulators with coupled friction”, in *Proc. IEEE Conference on Intelligent Robots and Systems*, Nice, France, Sep. 2008, pp. 3021-3027.

Paper III

Citation:

E. Naerum, H.H. King and B. Hannaford, "Robustness of the Unscented Kalman Filter for state and parameter estimation in an elastic transmission", in *Proc. Robotics: Science and Systems*, Seattle, WA, USA, Jun. 2009.

Paper IV

Citation:
E. Naerum and B. Hannaford, “Global transparency analysis of the Lawrence teleoperator architecture”, in *Proc. IEEE Conference on Robotics and Automation*, Kobe, Japan, May 2009, pp. 4344-4349.

Paper V

Citation:
E. Naerum, O.J. Elle and B. Hannaford, “The effect of interaction force estimation on performance in bilateral teleoperation”, *IEEE Transactions on Haptics*, accepted for publication.

Paper VI

Citation:
E. Naerum, B. Hannaford and O.J. Elle, "Force estimation and sensitivity optimization in teleoperated robotic surgery", *IEEE Transactions on Biomedical Engineering*, submitted for publication.

Paper VII

Citation:
E. Naerum, B. Hannaford and O.J. Elle, "Force sensor free bilateral teleoperation for robotic surgery - feasibility evaluation through human perception test", in *Proc. The Hamlyn Symposium on Medical Robotics*, London, United Kingdom, May 2010, pp. 25-26.

Errata

- On page vi: Entry for “Bibliography” added to the Table of Contents
- On page 14: “The only inputs to the UKF **are** the motor-side angle q_{m3} and the motor torque τ_{c3}.”
- On page 17: “The teleoperator’s telepresence properties describes to what extent the operator feels present at the remote site, and it is evaluated by seeing how well the master force f_m and velocity v_m match their respective quantities f_s and v_s on the slave side [99, 55].”
- On page 34: “It is difficult to attain a sensitivity that is not lower than that of direct manipulation. Optimization constraints that guarantee stability and well-behaving interaction force estimates reduces the attainable sensitivity.”